TacSuit: A Wearable Large-Area, Bioinspired Multimodal Tactile Skin for Collaborative Robots

Yanmin Zhou, *Member, IEEE*, Jiangang Zhao, Ping Lu, Zhipeng Wang, and Bin He, *Member, IEEE*

***Abstract*—Robots are now working more and more closely with humans outside of traditional fences in industrial scenes. Their real-time tactile interaction perception is crucial to the safety of human–robot collaboration (HRC). In this work, we present a customized, wearable, and modular robot skin (TacSuit), which is scalable for large-area surface coverage of robot with easily accessible multimodal sensors, including pressure, proximity, acceleration, and temperature sensors. The TacSuit is co-designed for mechanical structure and data fusion algorithm, consisting of three levels of design: sensor, cell (of multimodal sensors), and block (of multiple cells). These sensors are stored with custom-designed and 3-D printed capsules to achieve the conformity, scalability, and easy installation to the arbitrary robot surface. A multilevel event-driven data fusion algorithm enables efficient information processing for large number of tactile sensors. Furthermore, a virtual interaction force fusion method takes both the proximity and force perception information into consideration in order to achieve safety of whole interaction process before and after direct physical contacts. A humanoid robotic platform successfully realizes the TacSuit wear of 159 tactile cells. Validation experiments of obstacle detection demonstrate the effective collision avoidance capability of the TacSuit for safe HRC.**

***Index Terms*—Customed 3-D printing, human–robot collaboration (HRC), interaction safety, structure-algorithm co-design, wearable robot skin.**

I. Introduction

ROBOTS are now working increasingly closer with humans, and playing an important role in areas such as industry, medical care, and education [1]. They are no longer limited to isolated preprogrammed repeated tasks but interact with the environment, humans and other robots cooperatively. Therefore, safety, as an essential prerequisite, is crucial to the real-time perception of interaction [1]. Tactile perception is a necessary complement to the widely used vision perception of robots. It offers supplemental information of the environment, such as texture, softness, temperature, as well as the mechanical stimulations such as sliding, and vibration [2], [3]. On the other hand, the tactile perception is indispensable to tasks like delicate manipulation of robots [4].

The traditional force sensing of robot relays on the multiaxis force sensor at the end effector, and lacks for the whole body tactile sensing capabilities. E-skins provide the capabilities of large-area tactile sensing [5], [6]. It is an engineering imitation of human skin, which is embedded with many highly differentiated receptors [7], [8]. Robot E-skins can be generally grouped into two groups of soft robot skin and rigid robot skin. Their comparisons are summarized in Table I. Soft tactile skins for robots are normally made with intrinsic soft materials [9], [10]. The flexibility of these soft materials enables the skins to cover a variety of body shapes, including curved surfaces [11], [12]. The hard robot skins often employ industrially available sensors, such as barometers [13], temperature sensors [14], proximity sensors [15], [16], magnetic particles [17], [18], [19], and microphones [20]. They are commonly mounted on a PCB [21] or FPC [22]. These sensors are covered by some sort of soft shells [23] to provide the hard electric elements with certain softness and absorb the energy during bumping. It benefits from the signal processing technology of these off the shelf sensors, some of which even provide digital outputs directly [24].

It is very challenging to make one piece of robot skin to cover the whole surface of a robot [25]. Many humanoid robots only wear tactile sensors on the body parts that are frequently interacted with the environment, including the hand [26], arm [27], [28], chest [29], and abdomen [30]. The variance of surface areas, shapes, and surface curvatures of the whole robot magnifies its implementation difficulty [31], [32].

The modularized small electronic skin provides the possibility of a large-area scalable robot skin with certain flexibility and arbitrary shape to cover a robot's surface. The first approach of modular robot skin has been introduced in 2008 [33]. This RoboSkin used triangular skin cells with 12 capacitive force sensors to integrate a skin network which could form arbitrary shape and size to deploy on non-flat surfaces. Modular E-skins often

Manuscript received 20 October 2022; revised 11 January 2023; accepted 28 February 2023. Date of publication 13 March 2023; date of current version 16 August 2023. This work was supported in part by the National Natural Science Foundation of China under Grant U2013602, Grant 61825303, and Grant 51975415, in part by the National Key Research and Development Program of China under Grant 2020AAA0108905, in part by the Science and Technology Commission of Shanghai Municipality under Grant 2021SHZDZX0100, Grant 22ZR1467100, and Grant 22QA1408500, and in part by the Fundamental Research Funds for the Central Universities under Grant 22120210547. *(Corresponding author: Bin He.)*

The authors are with the Department of Control Science and Engineering, College of Electronics and Information Engineering, Tongji University, Shanghai 201804, China, and also with the Frontiers Science Center for Intelligent Autonomous Systems, Shanghai 201210, China (e-mail: yanmin.zhou@tongji.edu.cn; 1930762@tongji.edu.cn; pinglu@tongji.edu.cn; wangzhipeng@tongji.edu.cn; hebin@tongji.edu.cn).

Color versions of one or more figures in this article are available at https://doi.org/10.1109/TIE.2023.3253921.

Digital Object Identifier 10.1109/TIE.2023.3253921

0278-0046 © 2023 IEEE. Personal use is permitted, but republication/redistribution requires IEEE permission.
See https://www.ieee.org/publications/rights/index.html for more information.

Authorized licensed use limited to: UNIVERSITY OF COLORADO. Downloaded on July 08,2024 at 19:12:06 UTC from IEEE Xplore. Restrictions apply.

TABLE I
COMPARISONS OF SOFT AND HARD ROBOT E-SKIN

	Soft E-skin	Hard E-skin
Advantages	high resolution with soft interaction interface large area and arbitrary shape coverage multiple physical stimuli sensing	easy access of various commercial sensing elements convenient for data processing (with digital sensor outputs) economic for robotic applications
Disadvantages	susceptible to wear, damage, and multi-layer delamination high cost and sophisticated fabrication procedures slow dynamic response due to the hysteresis of soft materials wiring complexity	low resolution bulky size with shells low surface coverage and complex installation wiring sensor integration, installation and overall softness
Research difficulties	material and device configuration optimization manufacture for large-scale and multifunctional skin data processing for large number of multi-modal perceptions	low resolution wiring complexity data processing for large number of multi-modal sensors
Applications	intimate human robot cooperation soft robots (integrated with sensing and driving properties)	collision detection small area tactile sensing of rigid robot

have the advantage of multi-modal sensor integration. In [34], Stiehl et al. proposed a sensitive skin, which was able to sense touch (electric fields and force), temperature (thermistors), kinesthetic information (potentiometers), and pain (a sharp reading in any sensor). They successfully covered a Huggable robot arm with a net total over the whole body of more than 1000 force, 400 temperature, and 9 electric field sensors. Another representative E-skin of this type was proposed by Cheng et al. from TUM [14]. They covered the surface of a H1 robot with 1260 modularized E-skin cells, each of which contained proximity, force, acceleration, and temperature sensor.

In order to optimize the coverage of the rigid modular electronic skin, the size and shape of a single skin unit has been studied. In [35], Maiolino et al. applied equilateral triangle sensing units with a side length of 30 mm to form a large-scale robot skin and covered the iCub and WAM arms. In [36], Mittendorfer and Cheng used a regular hexagon with a side length of 16.31 mm as their skin cell. Both triangles and hexagon can parquet a plane without holes. Hexagons are advanced in neighbor communication via links. Furthermore, the sensor's hexagonal structure facilitates data augmentation for deep learning-based algorithm due to its sixfold rotation symmetry [29]. In [14], Cheng et al. developed a hexagonal multimodal robot skin cell to form a large-area skin network. In order to be mounted on the rigid robot surface, these rigid sensing cells often sit on flexible mediums [21], [37]. Recent publications have taken the surface geometry into consideration for wearable properties of rigid robot skin. In [28], Massari et al. developed a curved E-skin following the curvature of a robot arm, resembling a human forearm. A robot's total-body coverage could then be achieved through modular patches. Heng et al. [38] took the advantage of 3-D printing to replicate the robot's surface topography and manufactured a wearable E-skin. By deploying all units on 3-D-printed molds, they fabricated a soft skin and integrate it on a YuMi's arm where the shapes and contour were complex.

The modular E-skin with spatially dense tactile cells enables a robot with high spatial tactile perception resolution. The robot would be able to discriminate and localize single contact or multiple contacts. It would also benefit the contact area detections of interactions. As introduced above, a rigid industrial robot can be updated with the perception of E-skins and work as collaborative robots with humans. The contacts with different areas might be recognized as different contact patterns encoding different interaction information during collaboration, such as small area contacts for finger taping or poking, and large area contacts for hand grasping or body leaning. However, when a large-area electronic skin is used to cover the most part or even the whole body of a robot, the amount of data generated by the sensor units becomes very huge with a lot of redundant data. Transducing all the data brings burden both to the communication and computation process of the entire system [25]. Therefore, bio-inspired event-driven method has been introduced to shift the information extraction from a centralized processing system to the sensors, i.e., using distributed architecture with edge computing rather than centralized architecture [39]. Such tactile receptors produce spike trains only if certain novel information is detected [40], [41], inspired by the biological neural system which is only active when a novel information is represented by events. The information transduction, transmission, and processing are based on the event generation rather than the traditional clock-driven systems following the Nyquist theorem [42], [43]. A simple example of the event-driven signaling concept for robot skin systems is based on the SoDP (Send-on-Delta Principle) [44], [45]. This approach requires a microprocessor for each skin cell, and does not relay on any special hardware or special skin cell network architecture [45]. Cheng et al. [43] successfully reduced the network bandwidth by up to 90% and the CPU usage by up to 60% with event-driven signal processing of their robot E-skin.

The information from the whole body tactile perception enables complex motion control of robots. Ohmura and Kuniyoshi [46] proposed a "whole body contact motion" of a humanoid robot. An adult-size humanoid successfully lifted a 30 kg box by considering the motor power and the skillful motions for lifting with tactile feedback. Advait et al. [47] constructed a controller with the model predictive control, which enabled a robot arm to reach in a clutter environment with whole-arm tactile sensing. In [48], the whole body grasping of large unknown objects is proposed by adopting a human-like strategy of pulling large and unknown objects with both arms to the chest. Apart from this motion strategy plan, Cheng et al. [49] conducted robot control by fusing the contact and pre-contact information of their event-driven large-scale tactile skin. It was realized by defining dynamic tasks following the operational space formulation.

Authorized licensed use limited to: UNIVERSITY OF COLORADO. Downloaded on July 08,2024 at 19:12:06 UTC from IEEE Xplore. Restrictions apply.

TABLE II
SENSOR PROPERTIES

Sensor	Model	Mechanism	Manufacture	Size (mm)
Pressure	FMAMSDXX025WC2C3	Piezoresistive	Honeywell, New Jersey, USA	5.0×5.0×2.7
Proximity	VCNL4010	Optical reflection measurement	Vishay, Pennsylvania, USA	3.95×3.95×0.75
Vibration	BMI160	6-axis accelerometer	BOSCH, Stuttgart, Germany	2.5×3.0×0.83
Temperature	HDC2010	Capacitive	Texas Instruments, Texas, USA	1.5×1.5×0.675

In this work, we present TacSuit, which is inspired by the human skin and is capable of large-area multimodal tactile perception. It is a systematic solution for the design theory and implementation of the E-skin for robots. The TacSuit is 3-D printed and complies to the topography of robot's surface. The modular design of sensing cell enables the scalable of the skin. The co-design of leveled data transmission and event-driven information fusion further paves the way for large number of tactile sensor perception. Interaction experiments demonstrate a significant reduction of data transmission. We propose a virtual interaction force based on the temporal and spatial proximity and pressure sensing information during interaction. In order to verify its safe interaction capability, we evaluate a TacSuit wearing robot's performance with three different control strategies: emergency stop, path return, and active avoidance. Experiments show that, with the advances of this E-skin, robots are able to sense multimodal environmental stimuli during the whole process of interaction, ensuring the interaction safety.

To sum up, the main contributions of this article are as follows.

1) We propose a structure and algorithm co-designed novel tactile sensing suit for collaborative robots with multimodal and easily accessible sensors, bioinspired by the bone-muscle structure of humans.
2) We propose the use of 3-D printing technique to achieve the conformal skin to the robot arm's surface, which can be simply clipped on.
3) We propose an event-driven multilevel data fusion pyramid to improve the information processing efficiency, reduce the system bandwidth and information processing load of large number of sensors.
4) We conduct experiments on intimate interactions to verify the application of safety control of such E-skin for collaborative robots.

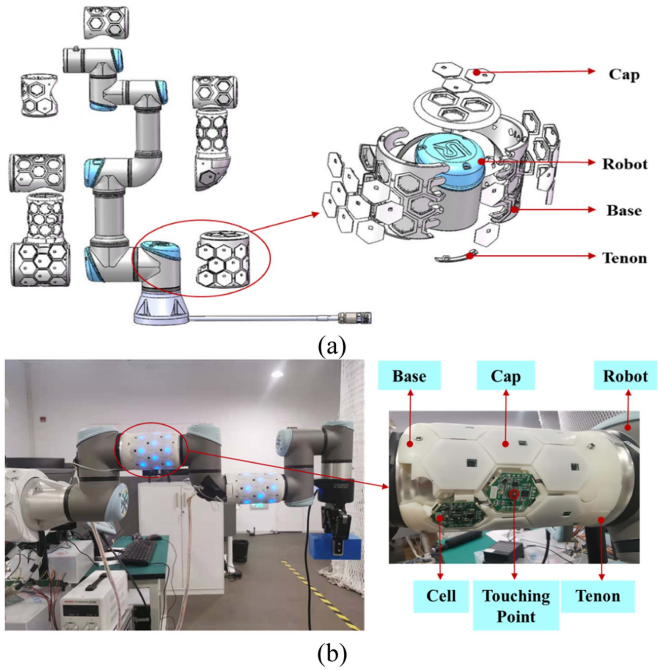

Fig. 1. Bone-muscle structure inspired multimodal E-skin. (a) Suit design of the skin with 3-D printing. (b) Mounting of the skin on the robot surface.

II. TACSUIT DESIGN

The proposed TacSuit for robots is inspired by the bone-muscle structure of human arm as shown in Fig. 1. The bone is the robot itself, which offers the system rigid but solid support and exerts powerful driving forces. The TacSuit is mounted on the surface of the bone, which consists of the tactile cells and the cell capsules. The tactile cell is constructed with multimodal tactile sensors, and a local computing MCU. The capsule is filled with and support the cells.

A. Tactile Cell

The presented tactile sensing cell is designed to mimic the human skin's tactile receptors by integrating off-the-shelf MEMS sensors. The proposed cell consists of four sensors for four types of tactile sensing, an MCU, and a power supply module. The sensors functionally emulate the tactile receptors of human hairy skins, including pressure, vibration, proximity, and temperature. Details of these sensors are shown in Table II. Besides, their price, dimension and data processing are considered to achieve cost effective and compact sensing module. The MCU regulates the working status of the sensors, collects and locally calculates the sensing data, and transmits the sensing information to the neighbor cell. The power supply module ensures the working power. The communication module connects and transmits the sensing information of modules to the PC.

B. Conformal TacSuit

The structure of the conformal TacSuit is demonstrated in Fig. 1, consisting of 3-D printed supporting bases, cell caps, and fixing tenons. The supporting base is the largest individual piece of a TacSuit. It carries storage units for a block of sensing cells on one side with wiring holes on the sidewalls connecting neighbor units. The caps are hexagonal in shape. Each cap has a square window for the light travel of the proximity sensor. The cap clips in the storage unit forming a capsule for the sensing cell. There is a protrusion from the inner base of the cap, which

Authorized licensed use limited to: UNIVERSITY OF COLORADO. Downloaded on July 08,2024 at 19:12:06 UTC from IEEE Xplore. Restrictions apply.

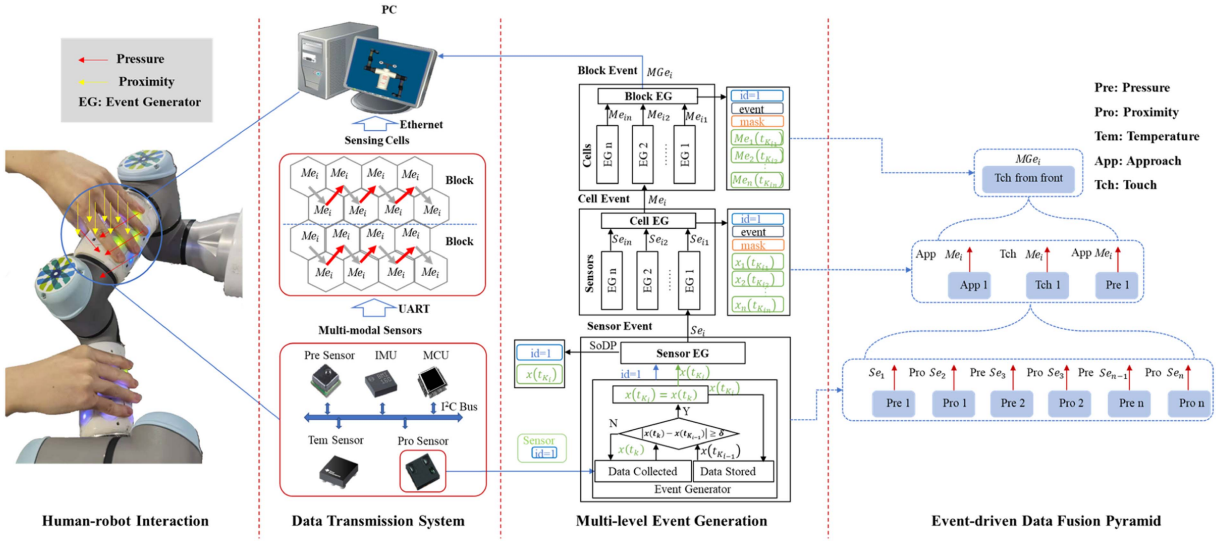

Fig. 2. Block diagram of the three-level event-driven data transmission system.

is right above the touching point of the pressure sensor on the sensing cell. The heights of this protrusion and the supporting pillars on the supporting base are designed in precision to make sure that the protrusion just touches the touching point of the pressure sensor for pressure transition. The outer side of the caps and the inner side of the supporting base are curved and copy the geometry of the robot making the TacSuit conformal. The connecting pieces of tenons connect supporting bases of the same region, and construct a complete piece of the suit [shown in Fig. 1(b)].

This proposed approach of wearable robot tactile skin requires no severe modifications to the robot, and can be easily scaled up to a full body skin. The TacSuit applies the advanced techniques of 3-D printing. It can be easily transformed to fit other robots once their surface geometry is known. More importantly, the structure and function are co-designed. Its fixed installation provides unique coordinates of sensing cells, which facilitates the interaction localizations. Meanwhile, the block connection of sensing cells agrees with the leveled event-driven data fusion and transmission greatly advancing the tactile sensing ability of the TacSuit as a whole.

C. Data Transmission

The sensing data is transferred to the PC via three-level transmission (see Fig. 2). The sensor data of one cell are collected by the MCU via I^2C before local processing. The data are then encoded and transferred to the neighbor cell via UART. Each cell adds its own data to those of the previous one and transfers them to the next cell, forming a sensing block. The last cell of a block contains all of its data, which are transferred to the ethernet module via UART. The ethernet module collects the data from all blocks and transfers them to the PC. The PC builds the socket connection with the TCP connection of the ethernet module via the TCP/IP protocols in order to obtain the server data of the real time sensing. Cells of the same block are connected serially. Blocks are then connected parallelly with the PC. Such series–parallel structured transmission design ensures the data collection of large number of sensors while maintaining a moderate complexity. This builds the data collection foundation for wearable E-skin for robotics with large area and large number of sensors.

III. Data Processing

A. Event-Driven

A full body covering TacSuit for robot consists of hundreds of cells, while each of them hosts multi sensors. Therefore, the effective data processing of large-area robot skin is challenging. Inspired by the human neural system, we propose an event-driven data processing algorithm. From the perspective of space and function, the TacSuit is designed with combination of modularization and hierarchical structure (see Fig. 2). Thus, a three-level event-driven data fusion system is proposed, including the sensor level, the cell level, and the block level. Each block contains a fixed number of cells, which are spatially close and connected by communication wires. The cell level event collects and fuses the sensor level events and transfers to that of the block level. Therefore, the number of events decreases from the sensor level, cell level to the block level successively forming a pyramid shape data fusion structure. The system bandwidth is reduced accordingly to ensure the effective data fusion and transmission. Meanwhile, this levelled event-driven algorithm takes advantages of the customized E-skin design. Each sensor's location on the robot surface is known as well as its ID. Furthermore, each block can be identified by its IP address communicating with the PC. Therefore, each sensor, cell, and block of a large-area E-skin can be identified with scalable capabilities. Such design facilitates the data fusion algorithm and the application of large-area E-skins.

In the sensor level, an MCU continually collects a sensor data. Instead of processing each clock-driven data, the MCU

Authorized licensed use limited to: UNIVERSITY OF COLORADO. Downloaded on July 08,2024 at 19:12:06 UTC from IEEE Xplore. Restrictions apply.

stores and transfers sensor events discretely, applying its local information processing abilities. It compares the current sensor data $x(t_{k_i})$ with the value $x(t_{k_{i-1}})$ of the previous event Se_{i-1}, and triggers a new event Se_i when their absolute difference is greater than the threshold δ. An event package contains the sensor *id* and $x(t_{k_i})$, and is sent based on SoDP. In the real scene application, the sensors on a same cell are often triggered synchronously by a same physical interaction from the human partner or the environment. Therefore, the communication cost reduction of the sensor level is limited. The advantage is that the sensor data can be locally processed by the MCU in order to smooth the data and reduce the impact of accidental abnormal data. The events of the sensor level are the inputs to the event generations of the next level.

In the cell level, all sensor events are packed into a public package, *i.e.*, cell event package, and to be fused to obtain higher level event. An event package Me_i contains the cell *id*, cell event description, and sensor *id*s set that generate the event mask, followed by the sensor level event $x(t_{k_i})$ of those sensors. Therefore, the size of the cell event package varies with the number of sensors that generate the event. Nevertheless, only one cell event package will be generated no matter how many sensors are stimulated, greatly reducing the transmission cost.

The block level event-driven data processing is designed based on the following considerations. For the TacSuit, the tactile cells are spatially close. In the cases of interactions with large objects, neighbor cells might be stimulated by the same physical interactions. The block level information fusion and event generation with multiple cells are very necessary.

As introduced above, the data of a block gathers to its last cell before they are transferred to the PC. Thus, the last cell of each block is driven by cell events Me_i and builds the fused block event MGe_i, including the block *id* (i.e., the IP address of the ethernet interface module), the fused block event, and the cell event values. The gathering cell of each block sends MGe_i to the PC via the TCP protocols, including event details of each level. The PC can then decode the event and generate control instructions to the robot. Therefore, each block could generate more extractive and high-level events by fusing the cell events. As the example shown in Fig. 2, an event of "touch from the front" can be generated once some cells on the front of the robot arm generate "touch" and "approach" events. Such leveled event-driven data fusion and transmission greatly enables the effective data fusion and transmission for scalable robot E-skin.

B. Threshold Adaptation

The event generation is crucial for an event-driven system. It needs to be sensitive to detect the interaction occurrence, but not too sensitive to avoid triggering events too frequently causing the data processing burden. The key is the threshold design. In this work, we design an adaptive threshold algorithm, which can be adopted to the requirements of application scenes.

The algorithm consists of two main steps: threshold initialization and threshold adaptation. First, we set the preliminary upper limit of the event generation rate, and determine the upper limit of the number of events allowed to occur per second and the minimum value of the preset threshold, according to the system bandwidth, data packet size, system load capacity, and noise sensitivity requirements. Then, the algorithm runs the initialization process based on the task, collects and selects the appropriate initialization threshold.

Algorithm 1: Threshold Adaptation.

Number of events $c = 0$, initialization threshold δ
Maximum event per second $C_{\max}$, preset minimum threshold $\delta_{\min}$
Sensor sampling rate k, value x, difference d
for $i = 1 : k$ **do**
    $d = |x_i - x_{i-1}|$
  if $d >= \delta$ **then**
    c++
  end
end
  if $c > C_{\max}$ **then**
increase δ
else if $c <$ a quarter of $C_{\max}$ **then**
        decrease δ
end if
if $\delta < \delta_{\min}$
  $\delta = \delta_{\min}$
end if

After initialization, the event-driven system of the E-skin runs according to the initialization threshold. The system counts the event rate in real time and compares it with the preset upper limit. Therefore, the threshold can be adapted on the basis of this comparison, ensuring that the event generation rate will not exceed the preset upper limit (see Algorithm 1).

C. Virtual Interaction Force

Considering the interaction safety, proximity and pressure sensors are the two main information sources. The proximity sensor detects approaching of human body or the environment before physical contacts. Once the contact occurs, the pressure sensor plays its role of contact force sensing while the proximity sensor reaches and maintains its maximum value. Meanwhile, the neighbor proximity sensors of the contact point will also detect the contact body, as shown in Fig. 2. In other words, the proximity and the pressure sensor play a combined role for the interaction perception of robots.

In this work, the proximity and pressure of the E-skin are fused into a virtual interaction force field. In this way, the interaction sensing range is greatly expanded spatially and temporally. Through the fusion of proximity and pressure, richer interaction information can be obtained (such as point or surface contact), facilitating the control of robot for interaction motions such as approaching, leaving, avoiding, and following.

Here, we propose a very straightforward fusion of the virtual force with the weighted summation of the proximity and pressure sensing values

$$F_z = \alpha_c F_c + \alpha_p F_p \tag{1}$$

Authorized licensed use limited to: UNIVERSITY OF COLORADO. Downloaded on July 08,2024 at 19:12:06 UTC from IEEE Xplore. Restrictions apply.

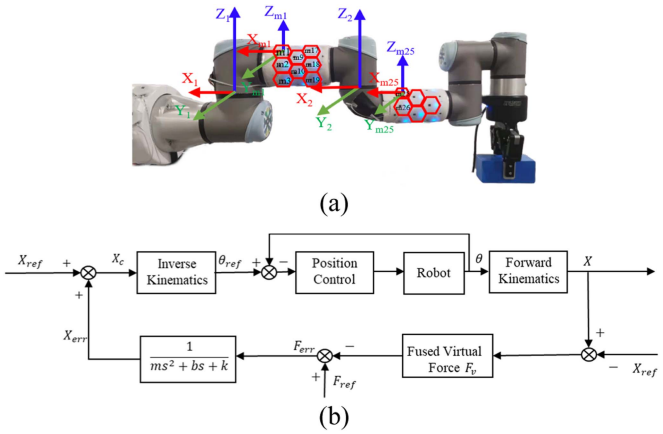

Fig. 3. Impedance control of the E-skin wearing robot arm. (a) Coordinate system of the E-skin cells. (b) Impedance control based on the fused virtual interaction force.

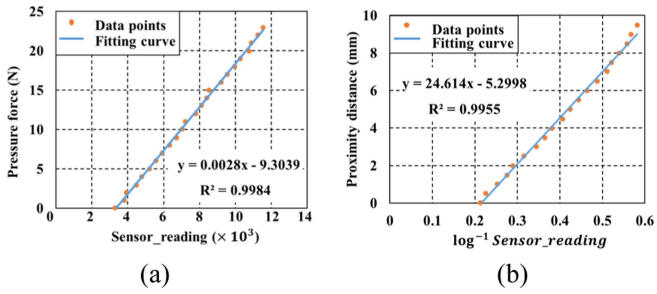

Fig. 4. Sensing properties of (a) the pressure sensor and (b) the proximity sensor.

where F_z, F_c, and F_p are the virtual force, pressure, and proximity value of a cell, while α_c and α_p are the weights of pressure and proximity values, respectively. The unit F_c of is N. F_p is the digital output of the proximity sensor, which is the response value of the sensor without unit of real physical meaning. Higher values indicate shorter distance to obstacles. Therefore, the virtual interaction force is without a unit of real physical meaning. The normal direction of cell i is selected as the positive direction of its virtual force. Thus, in its coordinate system $X_{mi} - Y_{mi} - Z_{mi}$, the virtual force vector can be written as follows:

$$F_i = \begin{bmatrix} 0 \\ 0 \\ F_z \end{bmatrix}. \tag{2}$$

The virtual force vector representation in the base coordinate system of the robot ${}^0F_i$ can then be achieved:

$${}^0F_i = {}^0T_{mi}\, F_i \tag{3}$$

where ${}^0T_{mi}$ is the transformation matrix of the robot's base coordinate system. The overall virtual interaction force of multiple cells is then calculated as the vector sum of the virtual interaction forces on all of the activated cells.

D. Compliance Control

In order to apply this virtual force to the robot control, it is necessary to build the kinematic model of the E-skin cells and the vector of the virtual force. The E-skin cells, that are mounted on the robot surface, have fixed positions. Therefore, their coordinate system can be easily achieved, as shown in Fig. 3(a). m_i is the cell *ID*, $i = 1, 2, 3, \ldots$, and $X_{mi} - Y_{mi} - Z_{mi}$ is its coordinate system.

As discussed above, multiple sensing cells are stimulated once an interaction occurs, which can be described by its position and virtual force vector. In this work, we apply the average coordinate and the virtual force vector as those of the fused virtual force F_v for these multiple cells. The joint control torque of the robot τ can be obtained

$$\tau = M(\theta)\ddot{\theta} + h\left(\theta, \dot{\theta}\right) - J^T(\theta)\left\{C_c\dot{P}_e + K_cP_e - F_v\right\}. \tag{4}$$

The compliance control of the robot based on the fused virtual interaction force can then be achieved, as shown in Fig. 3(b). X_{ref}, X_c, and X are the reference, control, and environment position trajectory of the robot, F_{ref} and F_v are the expected and fused virtual interaction force, respectively. The impedance model converts the force deviation $F_{\text{err}} = F_{\text{ref}} - F_v$ into the position deviation X_{err}. The PID controller realizes the position tracking of the inner loop. The position changes result in new F_v. Therefore, a closed loop control is formed for the impedance control based on the virtual contact force.

IV. Results

A. Wearable Robot E-Skin

The tactile sensing cell of our TacSuit E-skin is hexagonal with the side length of 15 mm, carrying the multiple tactile sensors. The pressure sensor locates at the center of the hexagon, and is the highest among all components in order to receive the direct physical contact force transferred from the cap. The square window on each cap allows the light of the proximity sensor to pass through for perception. Experiments show that the both of these two sensors can accomplish their perception tasks in this installation (see Fig. 4).

Due to the module design of this E-skin, the supporting base can be designed once the geometrical dimensions are obtained. Therefore, TacSuit, a customized wearable tactile sensing suit, can be achieved for robots. In this study, we constructed a multiple tactile sensing system for a humanoid robotic platform consisting of two UR3 arms and a bio-inspired visual system, which are all connected by a human like upper body (see Fig. 5). We have fulfilled the wear of 159 cells forming 17 blocks with 656 sensors.

B. Event-Driven Data Fusion

We have conducted experiments to verify the effectiveness of the event-driven data fusion algorithms. We have adopted the adapted threshold algorithm, and set the initialized upper limit of the event rate $C_{\max} = 10$, the minimum thresholds for the pressure and proximity event as 0.2 and 1000, respectively.

Authorized licensed use limited to: UNIVERSITY OF COLORADO. Downloaded on July 08,2024 at 19:12:06 UTC from IEEE Xplore. Restrictions apply.

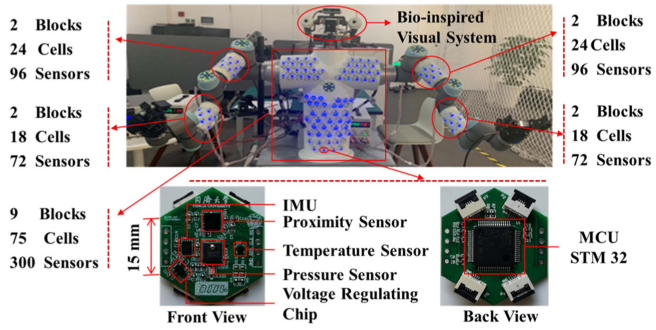

Fig. 5. Humanoid robotic platform wearing TacSuit tactile sensing E-skin.

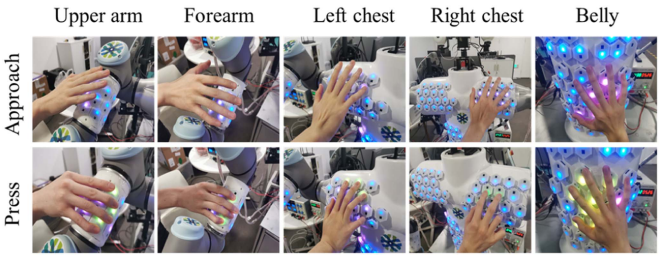

Fig. 6. Interaction between human hand and the humanoid robot body.

TABLE III
EXPERIMENTAL COMPARISONS OF THE TRANSFERRED DATA SIZES (KB) FOR BOTH CLOCK- AND EVENT-DRIVEN SYSTEMS

	Proximity				
	Upper arm	Forearm	Left chest	Right chest	Belly
Clock-driven	130.3	118.5	144.0	143.4	134.8
Event-driven	4.9	3.1	7.2	7.3	5.9
Reduction (%)	96.2	97.4	95.0	94.9	95.6
	Pressure				
	Upper arm	Forearm	Left chest	Right chest	Belly
Clock-driven	155.3	139.9	171.1	172.1	161.1
Event-driven	5.8	3.7	8.5	8.5	7.2
Reduction (%)	96.3	97.4	95.1	95.1	95.5

Data of the clock-driven system consist of sensor IDs and their values. All sensor data are sent to the PC. For the event-driven system, the PC receives the block level event package, including the block ID, a mask of the cells number and IDs that generate the event, and the cell level events. Each cell level event carries the sensor numbers, IDs and values that forming the cell level event.

Five repeated interaction experiments ($N = 50$) are carried out for both clock- and event-driven system, including both approaching (LED in red) and pressing (LED in green) (as shown in Fig. 6). The data size of each five experiments of the same type are averaged to minimize the experiment variations. As shown in Table III, for the same human interactions, the event-driven system can greatly reduce the data transmission by 95%. We should bear in mind that the degree of data transmission reduction depends seriously on the interaction type and frequency. Nevertheless, with the increase of sensor number of large-area robot E-skin, our proposed event-driven system can effectively reduce the redundant data transmission and promote the transmission efficiency.

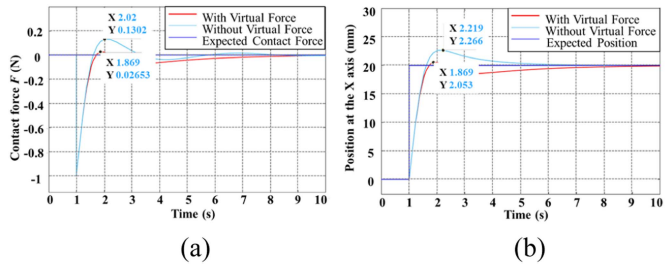

Fig. 7. Simulation results of the (a) contact force and (b) position of a robot end effector controlled by the same impedance model with or without the virtual force.

C. Safe Interaction

In order to verify the effectiveness of our proposed compliance control algorithm based on virtual forces, both simulation and physical experiments are carried out. For the simulation experiments, a robot arm is controlled to move from 0 to 20 mm along the X-axis, with the expected contact force of 0. Simulations are conducted with the same impedance model of the same parameters with or without the virtual force. As shown in Fig. 7, the robot end reaches the expected position with 0 force for both situations. However, the employment of the virtual force reduces the system overshoot, thereby avoiding the damage between the robot arm and the environment and improve the interaction safety of the system.

As shown in Fig. 8, physical interaction experiments were conducted with strategies of emergency stop, return along the original path and active avoidance in the contact direction. The initial motion trajectories of the manipulator keep the same. A fixed obstacle of the size of 130 × 65 × 10 mm was set in the path. Since the size of the tactile sensing cell of the TacSuit E-skin is much smaller than that of the obstacle, multiple cells are activated during the experiments. The critical value of contact is set as 7, which corresponds to $\alpha_c = 1$ and $\alpha_p = 0.2$ of (1). This is the situation of just and slight contact between the arm and the obstacle in order to be as close to the safe interaction in real applications as possible.

As shown in Fig. 9, for the emergency stop strategy, the force settles near the critical value, indicating the existence of virtual contact. For the rest two strategies, the robot arm leaves the obstacle and achieves the zero contact force. The virtual force decreases faster for the active avoidance than that of the path return strategy. The robot arm actively avoids contact along the direction of the virtual force, and costs least time to reach the zero contact force (see Table IV) benefiting the quick collision avoidance.

Authorized licensed use limited to: UNIVERSITY OF COLORADO. Downloaded on July 08,2024 at 19:12:06 UTC from IEEE Xplore. Restrictions apply.

Fig. 8. Snapshots on the physical interaction experiments with the control strategies of (a) emergency stop, (b) path return, and (c) active avoidance in the contact direction. yellow arrows in (c) indicate the contact force direction.

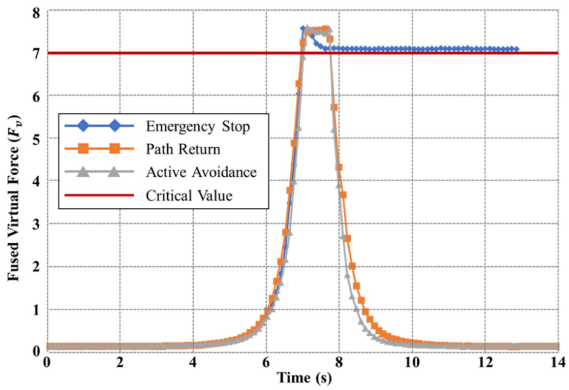

Fig. 9. Plots of the fused virtual force during physical interaction experiments.

TABLE IV
TIME SPENT COMPRISON OF DIFFERENT STRATEGIES

Strategy	Peak value	Time to peak/s	Time to 0/s
Emergency stop	7.569	7	/
Path return	7.523	7.375	3.875
Active avoidance	7.584	7.125	3.125

V. CONCLUSION

In this work, we presented a systematic solution for the design and implementation of a scalable and wearable TacSuit robot E-skin for the safe human–robot collaboration (HRC). This skin is mechanical in structure and data fusion algorithm co-designed, thereby achieving the scalability of both. TacSuit employs pressure, proximity, temperature, and acceleration sensors to perceive multimodal tactile interaction information. We applied 3-D printing technology to achieve conformal E-skin for arbitrary robot surface, which could be scaled to large area and whole body coverage of robot with minor parameter adjustments. On a self-built humanoid robot, we successfully fulfilled the wear of 159 tactile perception cells on its arms, shoulders, abdomen, and belly. In order to cope with the data processing of a large number of multimodal sensors, a multilevel event-driven data fusion algorithm was proposed. Our interaction experiments demonstrate a data transmission reduction by 95% compared with traditional clock-driven method. We further propose a virtual interaction force fusion method based on the temporal and spatial proximity and pressure sensing information during interaction before and after direct physical contact. Safe interaction experiments with a robot arm wearing the TacSuit were conducted with three different control strategies of emergency stop, path return, and active avoidance. Results showed that robots are able to perceive the obstacle on the moving path and maintain interaction safety with the feedback of this E-skin. TacSuit uses easily accessible commercial sensors and 3-D printing technology to construct wearable multimodal E-skin for robots. This TacSuit E-skin can be easily adopted by other robots. An industrial robot integrated with TacSuit can possess not only its original accurate and powerful executive capacity, but also multimodal tactile perception ability, similar to that of the human bone-skin structure.

In future work, the E-skin could be further optimized for better performances. The data transmission structure could be further modified to ensure safe data transmission. Currently, the serial connection of the cells of each block may cause a problem with data transmission when one cell or block is broken. For the future, the cells of the same region of the skin could be distributed to different blocks rather than the same block. Therefore, the failure of one cell or block will not lead to the complete loss of sensing ability of a whole area. A considerable number of sensors is used in our E-skin. The cost of the sensors should then be considered. Overall, the pressure sensor counts for over three quarters of the total cost of these sensors. Therefore, cheaper alternatives of the pressure sensor would help to reduce the cost. At present, the TacSuit consists of same cells with the same types of sensors. For the perception requirements during practical HRC applications in the future, cells with different sensor combination patterns could be applied. For example, less sensors would be enough for the areas with less interaction perception requirements. Such optimization would advance the cost control of the skin. The data fusion with more modalities of sensors would increase the interaction recognition and task execution capabilities of the robot. Apart from the pressure and proximity sensors of the skin, the acceleration and temperature sensors would be indispensable to tasks like self-modeling and

Authorized licensed use limited to: UNIVERSITY OF COLORADO. Downloaded on July 08,2024 at 19:12:06 UTC from IEEE Xplore. Restrictions apply.

temperature perception of the environment, which will be studied in the future.

REFERENCES

[1] N. Yogeswaran et al., "New materials and advances in making electronic skin for interactive robots," *Adv. Robot.*, vol. 29, no. 21, pp. 1359–1373, 2015, doi: 10.1080/01691864.2015.1095653.

[2] R. S. Dahiya, G. Metta, M. Valle, and G. Sandini, "Tactile sensing—From humans to humanoids," *IEEE Trans. Robot.*, vol. 26, no. 1, pp. 1–20, Feb. 2010.

[3] B. Heyneman and M. R. Cutkosky, "Slip classification for dynamic tactile array sensors," *Int. J. Robot. Res.*, vol. 35, no. 4, pp. 404–421, 2016, doi: 10.1177/0278364914564703.

[4] C. Bartolozzi, N. Lorenzo, and M. Giorgio, "Robots with a sense of touch," *Nature Mater.*, vol. 15, pp. 921–925, 2016, doi: 10.1038/nmat4731/.

[5] G. B. Avanzini, N. M. Ceriani, A. M. Zanchettin, P. Rocco, and L. Bascetta, "Safety control of industrial robots based on a distributed distance sensor," *IEEE Trans. Control Syst. Technol.*, vol. 22, no. 6, pp. 2127–2140, Nov. 2014.

[6] S. Robla-Gomez, V. M. Becerra, J. R. Llata, E. Gonzalez-Sarabia, C. Torre-Ferrero, and J. Perez-Oria, "Working together: A review on safe human-robot collaboration in industrial environments," *IEEE Access*, vol. 5, pp. 26754–26773, 2017.

[7] M. T. Almansoori, X. Li, and L. Zheng, "A brief review on E-skin and its multifunctional sensing applications," *Curr. Smart Mater.*, vol. 4, pp. 3–14, 2019, doi: 10.2174/2405465804666190313154903.

[8] M. L. Hammock, A. Chortos, B. Tee, J. Tok, and Z. A. Bao, "25th anniversary article: The evolution of electronic skin (E-skin): A brief history, design considerations, and recent progress," *Adv. Mater.*, vol. 25, no. 42, pp. 5997–6037, 2013, doi: 10.1002/adma.201302240.

[9] Y. Yamada, T. Morizono, Y. Umetani, and H. Takahashi, "Highly soft viscoelastic skin with a contact object-location-sensing capability," *IEEE Trans. Ind. Electron.*, vol. 52, no. 4, pp. 960–968, Aug. 2005.

[10] B. He, Y. M. Zhou, Z. P. Wang, Q. G. Wang, R. J. Shen, and S. Q. Wu, "A multi-layered touch-pressure sensing ionogel material suitable for sensing integrated actuations of soft robots," *Sens. Actuators A, Phys.*, vol. 272, pp. 341–348, 2018, doi: 10.1016/j.sna.2018.01.035.

[11] S. Gandla et al., "Ultrafast prototyping of large-area stretchable electronic systems by laser ablation technique for controllable robotic arm operations," *IEEE Trans. Ind. Electron.*, vol. 69, no. 4, pp. 4245–4253, Apr. 2022.

[12] R. Dahiya et al., "Large-area soft E-skin: The challenges beyond sensor designs," *Proc. IEEE*, vol. 107, no. 10, pp. 2016–2033, Oct. 2019.

[13] Y. Tenzer, L. P. Jentoft, and R. D. Howe, "The feel of MEMS barometers inexpensive and easily customized tactile array sensors," *IEEE Robot. Automat. Mag.*, vol. 21, no. 3, pp. 89–95, Sep. 2014.

[14] G. Cheng, E. Dean-Leon, F. Bergner, J. R. G. Olvera, Q. Leboutet, and P. Mittendorfer, "A comprehensive realization of robot skin: Sensors, sensing, control, and applications," *Proc. IEEE*, vol. 107, no. 10, pp. 2034–2051, Oct. 2019.

[15] T. D. Nguyen, T. Kim, J. Noh, H. Phung, G. Kang, and H. R. Choi, "Skin-type proximity sensor by using the change of electromagnetic field," *IEEE Trans. Ind. Electron.*, vol. 68, no. 3, pp. 2379–2388, Mar. 2021.

[16] D. Hughes, J. Lammie, and N. Correll, "A robotic skin for collision avoidance and affective touch recognition," *IEEE Robot. Automat. Lett.*, vol. 3, no. 3, pp. 1386–1393, Jul. 2018.

[17] H. B. Sun and G. Martius, "Guiding the design of superresolution tactile skins with taxel value isolines theory," *Sci. Robot.*, vol. 7, no. 63, pp. 1–12, 2022, doi: 10.1126/scirobotics.abm0608.

[18] Y. C. Yan et al., "Soft magnetic skin for super-resolution tactile sensing with force self-decoupling," *Sci. Robot.*, vol. 6, no. 51, pp. 1–12, 2021, doi: 10.1126/scirobotics.abc8801.

[19] R. M. Bhirangi, T. L. Hellebrekers, C. Majidi, and A. Gupta, "ReSkin: Versatile, replaceable, lasting tactile skins," in *Proc. 5th Annu. Conf. Robot Learn.*, 2021, pp. 1–11, doi: 10.48550/arXiv.2111.00071.

[20] M. J. Yang, K. Park, and J. Kim, "A large area robotic skin with sparsely embedded microphones for human-robot tactile communication," in *Proc. IEEE Int. Conf. Robot. Automat.*, 2021, pp. 3248–3254.

[21] S. Tsuji and T. Kohama, "Proximity and contact sensor for human cooperative robot by combining time-of-flight and self-capacitance sensors," *IEEE Sens. J.*, vol. 20, no. 10, pp. 5519–5526, May 2020.

[22] E. Cheung and V. Lumelsky, "A sensitive skin system for motion control of robot arm manipulators," *Robot. Auton. Syst.*, vol. 10, no. 1, pp. 9–32, 1992, doi: 10.1016/0921-8890(92)90012-N.

[23] T. D. Nguyen et al., "Highly sensitive flexible proximity tactile array sensor by using carbon micro coils," *Sens. Actuators A, Phys.*, vol. 266, pp. 166–177, 2017, doi: 10.1016/j.sna.2017.09.013.

[24] L. P. Jentoft, Y. Tenzer, D. Vogt, J. Liu, R. J. Wood, and R. D. Howe, "Flexible, stretchable tactile arrays from MEMS barometers," in *Proc. 16th Int. Conf. Adv. Robot.*, 2013, pp. 1–6, doi: 10.1109/ICAR.2013.6766525.

[25] R. S. Dahiya, P. Mittendorfer, M. Valle, G. Cheng, and V. J. Lumelsky, "Directions toward effective utilization of tactile skin: A review," *IEEE Sens. J.*, vol. 13, no. 11, pp. 4121–4138, Nov. 2013.

[26] Z. Kappassov, J. A. Corrales, and V. Perdereau, "Tactile sensing in dexterous robot hands - Review," *Robot. Auton. Syst.*, vol. 74, pp. 195–220, 2015, doi: 10.1016/j.robot.2015.07.015.

[27] L. Van Duong and V. A. Ho, "Large-scale vision-based tactile sensing for robot links: Design, modeling, and evaluation," *IEEE Trans. Robot.*, vol. 37, no. 2, pp. 390–403, Apr. 2021.

[28] L. Massari et al., "Functional mimicry of Ruffini receptors with fibre Bragg gratings and deep neural networks enables a bio-inspired large-area tactile-sensitive skin," *Nature Mach. Intell.*, vol. 4, no. 5, 2022, Art. no. 425, doi: 10.1038/s42256-022-00487-3.

[29] D. P. Kong et al., "Bioinspired co-design of tactile sensor and deep learning algorithm for human-robot interaction," *Adv. Intell. Syst.*, vol. 4, no. 6, 2022, Art. no. 2200050, doi: 10.1002/aisy.202200050.

[30] N. Mitsunaga, T. Miyashita, H. Ishiguro, K. Kogure, and N. Hagita, "Robovie-IV: A communication robot interacting with people daily in an office," in *Proc. IEEE/RSJ Int. Conf. Intell. Robots Syst.*, 2006, pp. 5066–5072.

[31] T. Minato, Y. Yoshikawa, T. Noda, S. Ikemoto, H. Ishiguro, and M. Asada, "CB2: A child robot with biomimetic body for cognitive developmental robotics," in *Proc. 7th IEEE-RAS Int. Conf. Humanoid Robots*, 2007, pp. 557–562.

[32] C. R. Liu, C. T. Ishi, H. Ishiguro, and N. Hagita, "Generation of nodding, head tilting and gazubg for huamn-robot speech interaction," *Int. J. Humanoid Robot.*, vol. 10, no. 1, 2013, Art. no. 13500096, doi: 10.1142/S0219843613500096.

[33] G. Cannata, M. Maggiali, G. Metta, and G. Sandini, "An embedded artificial skin for humanoid robots," in *Proc. IEEE Int. Conf. Multisens. Fusion Integr. Intell. Syst.*, 2008, pp. 434–438.

[34] W. D. Stiehl et al., "The huggable: A therapeutic robotic companion for relational, affective touch," in *Proc. 3rd IEEE Consum. Commun. Netw. Conf.*, 2006, pp. 1290–1291.

[35] P. Maiolino, M. Maggiali, G. Cannata, G. Mettaet, and L. Natale, "A flexible and robust large scale capacitive tactile system for robots," *IEEE Sens. J.*, vol. 13, no. 10, pp. 3910–3917, Oct. 2013.

[36] P. Mittendorfer and G. Cheng, "Humanoid multimodal tactile-sensing modules," *IEEE Trans. Robot.*, vol. 27, no. 3, pp. 401–410, Jun. 2011.

[37] D. Kim, S. Han, T. Kim, C. Kim, and J. S. Koh, "Design of a sensitive balloon sensor for safe human-robot interaction," *Sensors-Basel*, vol. 21, no. 6, 2021, Art. no. 2163, doi: 10.3390/s21062163.

[38] W. Z. Heng, G. Yang, G. Y. Pang, Z. Q. Ye, and Z. B. Pang, "Fluid-driven soft CoboSkin for safer human-robot collaboration: Fabrication and adaptation," *Adv. Intell. Syst.*, vol. 3, no. 3, 2021, Art. no. 2000038, doi: 10.1002/aisy.202000038.

[39] E. P. Gardner and K. O. Johnson, *Principles of Neural Science*, 5th ed. New York, NY, USA: McGraw-Hill, 2013, ch. 23, pp. 498–529.

[40] F. Bergner, E. Dean-Leon, and G. Cheng, "Event-based signaling for large-scale artificial robotic skin - Realization and performance evaluation," in *Proc. IEEE/RSJ Int. Conf. Intell. Robots Syst.*, 2016, pp. 4918–4924.

[41] F. Bergner, E. Dean-Leon, J. R. Guadarrama-Olvera, and G. Cheng, "Evaluation of a large scale event driven robot skin," *IEEE Robot. Automat. Lett.*, vol. 4, no. 4, pp. 4247–4254, Oct. 2019.

[42] G. Arren, V. Valentina, I. Massimiliano, and B. Chiara, "The event-driven software library for YARP—With algorithms and iCub applications," *Front. Robot. AI*, vol. 4, 2018, doi: 10.3389/frobt.2017.00073.

[43] F. Bergner, E. Dean-León, and G. Cheng, "Efficient event-driven reactive control for large scale robot skin," in *Proc. IEEE Int. Conf. Robot. Automat.*, 2017, pp. 394–400.

[44] M. Neugebauer and K. Kabitzsch, "A new protocol for a low power sensor network," in *Proc. IEEE Int. Conf. Perform., Comput., Commun.*, 2004, pp. 393–399.

[45] M. Miskowicz, "Send-on-delta concept: An event-based data reporting strategy," *Sensors-Basel*, vol. 6, no. 1, pp. 49–63, 2006, doi: 10.3390/s6010049.

[46] Y. Ohmura and Y. Kuniyoshi, "Humanoid robot which can lift a 30 kg box by whole body contact and tactile feedback," in *Proc. IEEE/RSJ Int. Conf. Intell. Robots Syst.*, 2007, pp. 1136–1141.

Authorized licensed use limited to: UNIVERSITY OF COLORADO. Downloaded on July 08,2024 at 19:12:06 UTC from IEEE Xplore. Restrictions apply.

[47] A. Jain, M. D. Killpack, A. Edsinger, and C. C. Kemp, "Reaching in clutter with whole-arm tactile sensing," *Int. J. Robot. Res.*, vol. 32, no. 4, pp. 458–482, 2013, doi: 10.1177/0278364912471865.
[48] P. Mittendorfer, E. Yoshida, and G. Cheng, "Realizing whole-body tactile interactions with a self-organizing, multi-modal artificial skin on a humanoid robot," *Adv. Robot.*, vol. 29, no. 1, pp. 51–67, 2015, doi: 10.1080/01691864.2014.952493.
[49] O. Khatib, "A unified approach for motion and force control of robot manipulators - the operational space for mulation," *IEEE J. Robot. Automat.*, vol. 3, no. 1, pp. 43–53, Feb. 1987.

Yanmin Zhou (Member, IEEE) received the M.S. degree in control theory and control engineering from Tongji University, Shanghai, China, in 2011, and the Ph.D. degree in biomechanics from Cambridge University, Cambridge, U.K., in 2015.

She is currently a Vice Professor with the Department of Control Science and Engineering, College of Electronics and Information Engineering, Tongji University. Her current research interests include bionics, the design and control of intelligent robot.

Jiangang Zhao received the B.S. degree in automation from Donghua University, Shanghai, China, in 2019, and the M.S. degree in control science and engineering from the Department of Control Science and Engineering, College of Electronics and Information Engineering, Tongji University, Shanghai, China, in 2022.

His current research interests include electric-skin and robot safety control.

Ping Lu received the graduate degree in automation from Tongji University, Shanghai, China, in 2006.

She pursued doctor program in Friedrich-Alexander-Universität Erlangen-Nürnberg, Nuremberg, Germany, from 2006 to 2013. She is currently a research employee with Tongji University. Her research interests include robotic sensing theory and technology.

Zhipeng Wang received the M.S. degree in mechanical engineering from Zhejiang University, Hangzhou, China, in 2011, and the Ph.D. degree in mechanical engineering from Tongji University, Shanghai, China, in 2015.

Between 2015 and 2018, he held postdoctoral research appointments with the College of Mechanical Engineering, Tongji University. He is currently a Vice Professor with the Department of Control Science and Engineering, College of Electronics and Information Engineering, Tongji University. His current research interests include biped robot, mechatronics, and dynamics.

Bin He (Member, IEEE) received the B.S. degree in engineering machinery from Jilin University, Changchun, China, in 1996, and the Ph.D. degree in mechanical and electronic control engineering from Zhejiang University, Hangzhou, China, in 2001.

He held postdoctoral research appointments with The State Key Lab of Fluid Power Transmission and Control, Zhejiang University, from 2001 and 2003. He is currently a Professor with the Department of Control Science and Engineering, College of Electronics and Information Engineering, Tongji University, Shanghai, China. His current research interests include intelligent robot control, biomimetic microrobots, and wireless networks.

Authorized licensed use limited to: UNIVERSITY OF COLORADO. Downloaded on July 08,2024 at 19:12:06 UTC from IEEE Xplore. Restrictions apply.